

Gas Transport Properties of Poly(2-ethoxyethyl methacrylate-*co*-2-hydroxyethyl methacrylamide)

P. Tiemblo,^{*,†} M. F. Laguna,[†] F. García,[‡] J. M. García,[‡] E. Riande,[†] and J. Guzmán[†]

Instituto de Ciencia y Tecnología de Polimeros (CSIC), Calle Juan de la Cierva 3, 28006 Madrid, Spain, and Universidad de Burgos, Plaza Misael Bañuelos s/n, 09001 Burgos, Spain

Received January 8, 2004; Revised Manuscript Received March 12, 2004

ABSTRACT: A series of methacrylic copolymers was prepared by radical polymerization of the monomers 2-ethoxyethyl methacrylate and 2-hydroxyethyl methacrylamide and a small quantity of a cross-linking agent ethylene glycol dimethacrylate. Water swelling of the membranes, mechanodynamical analysis, density measurements, and ATR-FTIR studies were performed on the copolymers. High vacuum pressure techniques were used to evaluate the flow of He, O₂, N₂, CO₂, CH₄, CH₃CH₃, and CH₂CH₂ through these membranes, and solubility, diffusivity, and permeability coefficients were determined. The effect of the increase of the amount of methacrylamide in the copolymer on transport properties, glass transition, fractional free volume, cohesive energy density, and specific interactions has been studied and is reported in this work.

Introduction

The development of polymeric materials with tailored properties requires both accurate knowledge on property–structure correlations and proficiency at synthesizing polymers with predetermined structures. In the field of species separation using polymeric membranes, a lot of work has been done during the last three decades in the synthesis of polymers with improved selectivity for given gases and vapors,^{1–4} in the development of better membrane technology,^{3,5–9} and in the opening of new research fields, such as facilitated transport for the separation of very similar species (O₂/N₂, paraffin/olefin), application of pervaporation for the separation of azeotropic mixtures, polymer gels containing ionic salts for ionic transport, etc.^{10,11} At this moment, areas of interest in membrane technology include, for instance, the ability of future membranes to operate in chemical, thermal, or pressure conditions under which they are unable now or the ability to separate very similar species. Polymeric based new materials in which inorganic or metallic components lead to the generation of new properties is one of the fields recently developing. In this context, a few years ago we began systematic research on the synthesis and gas transport properties of solid methacrylic polymers or copolymers in which the structure is varied in order to (i) obtain basic knowledge on the dependence of gas transport on the structure of the methacrylate and (ii) synthesize methacrylic polymers with tailored properties which can constitute the matrix of new membrane materials.

As we showed in previous work, the transport properties are strongly dependent on the side groups present in the methacrylate structure. To date we have studied the effect of introducing aliphatic¹² or oxyethylene¹³ side chains of increasing length; the polarity of these chains is very low, and the main effect of introducing these chains as side groups is the possibility to enhance flexibility and mobility and to lower the glass transition

of the resulting polymer. Thus, in the case of aliphatic side chains, increasing the length of the chain from 3 to 9 bonds lowers the T_g by almost 80 °C; similarly, when the number of bonds in the oxyethylene side chain increases from 3 to 9, the T_g is lowered by almost 100 °C. In both cases, then, at room temperature, polymers with long side chains are softer and more flexible and, in accordance, their diffusion coefficients higher than similar methacrylates with shorter pendant groups. An important finding on the structure–property relationship was that copolymers with units of different side chain length behaved in the same way as the corresponding homopolymer with the same average side chain length regarding both transport properties and T_g values.¹²

On the other hand, if the pendant group is not an oxyethylene linear chain but a crown ether with the same number of oxyethylene units, then flexibility is not attained and consequently T_g is not lowered and diffusion coefficients are not increased.¹⁴ We compared, in particular, the behavior of poly(1,4,7,10-tetraoxacyclododecan-2-yl)methacrylate and its linear chain analogue poly(2-[2-(2-ethoxyethoxy)ethoxy]ethyl methacrylate). These crown ether methacrylic polymers have the added interest of being able to coordinate metal ions in hydrophobic solvents, originating the separation from their associated anions and making their salts soluble in these solvents. The use of such compounds for species separation has been investigated recently.^{15–18} Particularly important is the possibility to develop membranes in which facilitated transport of oxygen takes place.^{19–22} As we have seen, the mechanical properties of these crown ether methacrylates are reasonable; they are not fragile, and easy to handle in the solid state, and therefore interesting in different transport fields.

One of the application fields in which methacrylate membranes can be successfully used is the development of water-swelled membranes able to diffuse oxygen readily. None of the methacrylic polymers studied by us to date could be used in such applications, as the apolarity of the structure does not allow the swelling in water to take place. The development of methacrylic polymers with polar side chains which absorb water was

* To whom correspondence should be addressed. E-mail: ptiemblo@ictp.csic.es.

[†] Instituto de Ciencia y Tecnología de Polimeros (CSIC).

[‡] Universidad de Burgos.

therefore envisaged. However, highly polar structures are also very often rigid, fragile, and difficult to handle in the solid state because of their poor mechanical properties. The copolymerization of monomers with long apolar side chains and monomers with highly polar pendant groups seems to be a solution to obtain methacrylic membranes which are both easy to handle in the solid state and readily form gels when swelled with water. In the following paper we present the results of two such copolymers, one prepared with 2,3-dihydroxypropyl methacrylate (MAG) and 2-ethoxyethyl methacrylate (EEMA) and the other with 2-hydroxyethyl methacrylamide (HEMAM) and 2-ethoxyethyl methacrylate. As will be shown, not all polar monomers are useful for our purposes and not all compositions of useful copolymers are of interest.

Experimental Section

1. Preparation and Characterization of the Membranes. Materials. Methacryloyl chloride, 2-aminoethanol, ethanedioldimethacrylate, 1,2-isopropylidenglycerol (IPG), and triethylamine (Fluka) were used as received. The commercial monomer 2-ethoxyethyl methacrylate (EEMA) (Aldrich, 99%) was purified by distillation under high vacuum. 2,2'-Azobisisobutyronitrile (AIBN, Fluka, 98%) was recrystallized from methanol and dried under high vacuum at room temperature.

Synthesis of the Monomers HEMAM and MAG. The monomer 2-hydroxyethyl methacrylamide (HEMAM) was prepared by adding dropwise methacryloyl chloride to 2-aminoethanol dissolved in an aqueous sodium hydroxide solution. The reaction was carried out at 0 °C under nitrogen atmosphere. The monomer was purified by means of several extractions with dichloromethane, obtaining a product with purity higher than 99%, as determined by high-performance liquid chromatography (HPLC) and gas chromatography.²³

The monomer 2,3-dihydroxypropyl methacrylate (MAG) was obtained by acid hydrolysis of their intermediate compound, isopropylidene methacrylate, which was previously prepared by reaction between methacryloyl chloride with 1,2-isopropylidenglycerol (IPG) in chloroform under nitrogen atmosphere and using triethylamine to neutralize hydrogen chloride evolved during the reaction. Methacryloyl chloride was added dropwise into the solution of IPG over a period of 30 min, and the reaction medium was kept cold with an ice-water bath. The triethylamine salt was removed by filtration, and the reaction mixture was washed several times with distilled water. Finally, the crude product was distilled under vacuum to give the monomer. The purity of all the compounds was checked by high-performance liquid chromatography (HPLC) and NMR.²⁴

Synthesis of the Copolymers (Membranes). The membranes were prepared by radical polymerization of a mixture of EEMA (ranging from 50 to 100 wt %) and MAG or HEMAM using 1,2-ethanedioldimethacrylate as cross-linking agent and AIBN (2.5 wt %) as initiator. The nominal cross-linking ratio, i.e., the ratio between the number of moles of monomer to the cross-linking agent, was 600 for MAG/EEMA membranes and 320 for HEMAM/EEMA membranes. The addition of a cross-linking agent is necessary in order to obtain membranes with adequate mechanical properties. The reaction was carried out in a silanized glass mould of 100 μm thickness in oxygen-free atmosphere at 70 °C for 5 h. The network was extracted three times in acetone/water (1/1) for a period of 72 h. Finally, the network was dried at room temperature for 1 week, and the residual solvent was eliminated under high vacuum at room temperature.

Copolymers made of 2-ethoxyethyl methacrylate and 2-hydroxyethyl methacrylamide will be called hereafter MM-X/Y, where X stands for the molar fraction of ethoxyethyl and Y stands for the molar fraction of methacrylamide. Copolymers made from 2-ethoxyethyl methacrylate and 2,3-dihydroxypro-

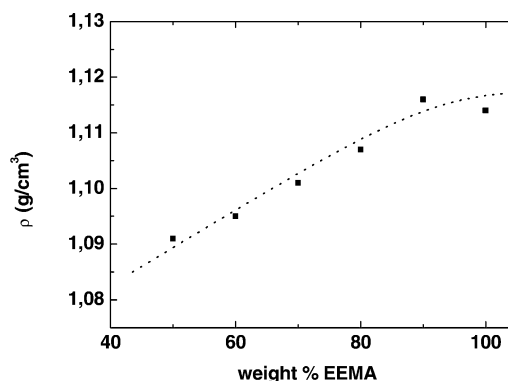


Figure 1. Density of copolymers as a function of their composition in membranes dried at 68 °C for 3 days.

Table 1. Physicochemical Characterization of the Copolymers

sample	EEMA molar %	T_g (°C) DMTA	ρ (g/cm ³)	FFV	swelling % H ₂ O uptake
PEEMA	100	-16	1.11 ₄	0.158	0.8
MM-90/10	90	47	1.11 ₆	0.162	2.7
MM-80/20	80	75	1.10 ₇	0.174	20.4
MM-70/30	70	99	1.10 ₁	0.180	52.4
MM-60/40	60	139	1.09 ₅	0.191	71.8
MM-50/50	50	189	1.09 ₁	0.195	152.7

pyl methacrylate will be called hereafter MG-X/Y, where X stands for the molar fraction of ethoxy ethyl and Y stands for the molar fraction of 2,3-dihydroxypropyl methacrylate.

2. Membrane Characterization. 2.1. Fractional Free Volume Estimation: Density Measurements. The density of the membranes derived was accomplished with a 5 mL Weld pycnometer device at 25 °C. A 200 mg amount of the proper membrane was introduced in the dried pycnometer, and the solvent was added to the device. The density, which appears in Figure 1 and Table 1, was obtained from the different weights of pure solvent and the solvent-membrane system.

The density values were used to estimate the fractional free volume (FFV) at 25 °C by applying

$$FFV = \frac{V - 1.3V_w}{V} \quad (1)$$

where V is the polymer specific volume and V_w is the specific van der Waals volume, which was estimated by using the Hyperchem computer program, version 5.01.²⁵

2.2. Relaxations and Transitions: Mechanodynamical Analysis. The mechanodynamical spectra of the copolymers were obtained with a Thermal Instrument DMA 983 analyzer in flexion mode from rectangular strips, typical dimension being 8 × 4 × 0.6 mm. The temperature dependence of the loss modulus was determined at 0.1 Hz, between -150 and 250 °C, at a heating rate of 5 °C min⁻¹, and using a deformation amplitude of 1 mm. Some selected spectra appear in Figure 2. Figure 3 shows the glass-transition temperature as a function of the weight percentage of EEMA.

2.3. Specific Interactions: ATR-FTIR. The composition and specific interactions in these copolymers have been studied by ATR-FTIR. The spectra were recorded on the membranes using a FTIR Perkin-Elmer Spectrum-One, 10 scans, and 2 cm⁻¹ resolution. The carbonyl region (1600–1800 cm⁻¹) and the 3000–4000 cm⁻¹ region are depicted in Figures 4 and 5, and will be discussed in the following sections.

3. Permeation Measurements. The same lab-made permeator as in former work²⁶ has been used. It consists of a gas cell in the middle of which the polymer membrane is placed. This membrane separates the upstream and downstream chambers. For simplified equations relating the gas flow through the membrane to the transport coefficients to be valid, the downstream pressure has to be kept very low, negligible as compared to the upstream. This is accomplished by thor-

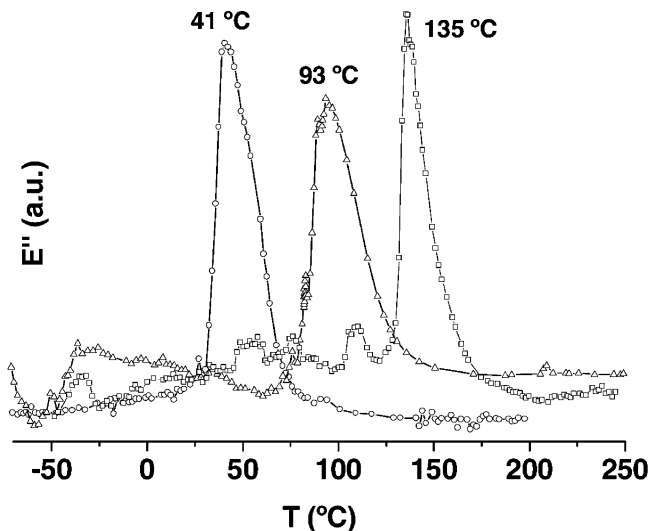


Figure 2. Mechanical analysis of copolymers MM-50/50 (○), MM-70/30 (△), and MM-90/10 (□) showing the glass transition.

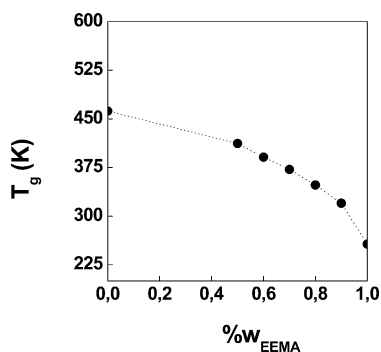


Figure 3. Glass-transition temperature as a function of the composition of the MM copolymers.

ough evacuation of the downstream pressure, prior to any measurement, by means of a Edwards turbomolecular pump. At the low-pressure side, a MKS Baratron type 627B absolute pressure transducer measures the pressure increase, while upstream a Gometrics pressure detector is used to control the gas pressure at which the experiment is performed. The Baratron 627B can be used in the pressure range $1-10^{-4}$ Torr. The Baratron is connected via a MKS power supply/readout unit to the PC, which records the pressure increase at given time intervals. The whole setup is temperature controlled in the range $5-80$ °C by means of a water bath.

Before measurements are performed, a vacuum is kept overnight in order to remove any residual solvent from the membrane and to attain a downstream pressure as low as possible. Prior to the permeation experiment, measurement of the pressure increase due to imperfect vacuum isolation of the downstream chamber is recorded. This blank experiment is then subtracted from the permeation experiment performed immediately afterward in order to calculate the gas transport coefficients from the corrected pressure curves. In this way the pressure increase is related solely to the gas diffusing across the membrane.

The permeability and diffusivity coefficients have been calculated from the curves measuring the pressure increase at the downstream. Equation 2, derived from integration of Fick's laws, relates the amount of diffusant per unit of area, $Q(t)$, traversing the membrane to the thickness of the membrane, l , to the concentration of diffusant at the upstream side of the membrane C_1 and to the diffusion coefficient D . In fact, only four terms of this equation are enough to correctly fit our flow curves.

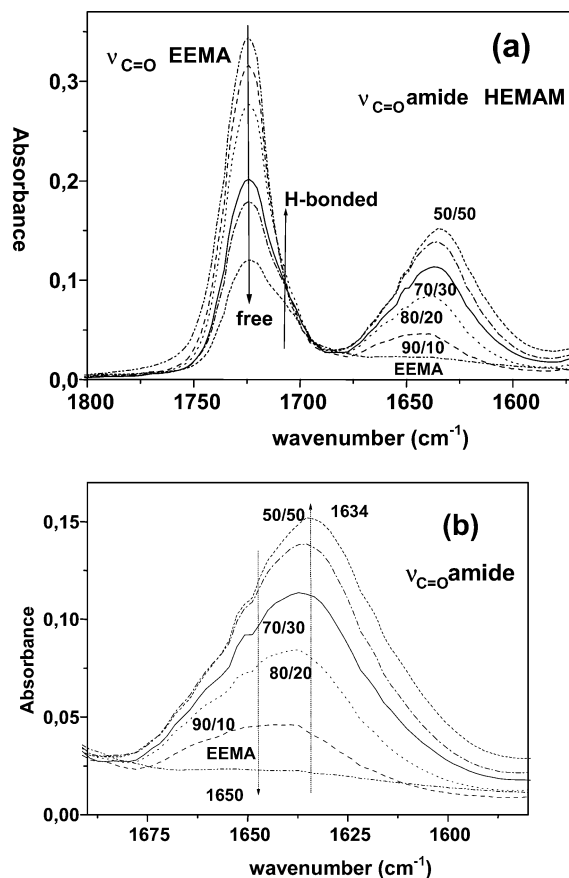


Figure 4. ATR-FTIR in the region $1600-1800$ cm^{-1} of the MM copolymers.

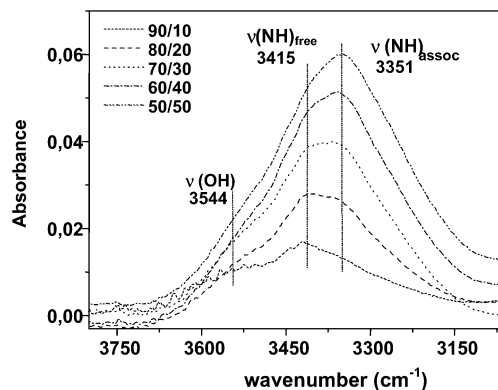


Figure 5. ATR-FTIR in the region $3000-3800$ cm^{-1} of the MM copolymers.

$$\frac{Q(t)}{lC_1} = \frac{Dt}{l^2} - \frac{1}{6} - \frac{2}{\pi^2} \sum_{n=1}^{\infty} \frac{(-1)^n}{n^2} e^{-Dn^2\pi^2 t/l^2} \quad (2)$$

The diffusion coefficient is directly obtained from the fitting, and the solubility coefficient is directly proportional to C_1 . The permeability P is obtained as $S \cdot D = P$. Calculation of the uncertainties in the diffusion coefficients has been performed in the following way

$$\sigma = 100 \frac{\left[\left| \frac{J\epsilon(l)}{3\theta} \right| + \left| \frac{J^2\epsilon(\theta)}{6\theta^2} \right| \right]}{D} \quad (3)$$

where θ is the time lag. Uncertainties in permeability and diffusivity are about 20% and 15%, respectively.

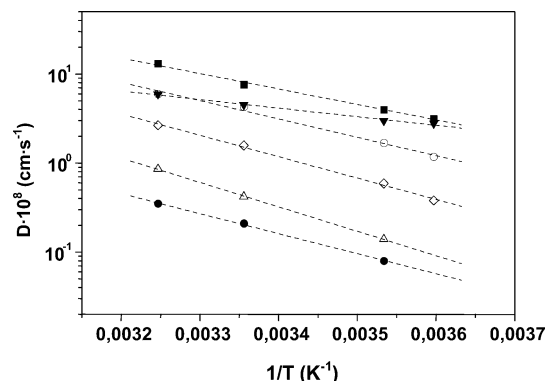


Figure 6. Diffusion coefficients of MM-70/30 in Arrhenius coordinates. The actual activation energies appear in Table 2. The code for gases is oxygen (■), nitrogen (○), methane (◇), carbon dioxide (▼), ethane (●), and ethylene (△).

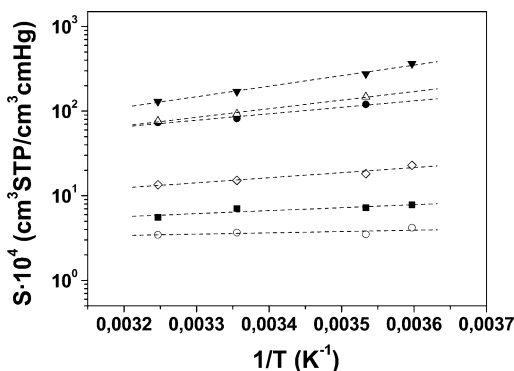


Figure 7. Solubility coefficients of MM-70/30 in Arrhenius coordinates. The actual heats of solution appear in Table 3. The code for gases is oxygen (■), nitrogen (○), methane (◇), carbon dioxide (▼), ethane (●), and ethylene (△).

Table 2. PEEMA and MM-70/30 Diffusion Activation Energies

gas	E_d (kJ mol ⁻¹) PEEMA	E_d (kJ mol ⁻¹) MM-70/30
O ₂	15	33
N ₂	18	39
CO ₂	19	18
CH ₄		46
CH ₂ CH ₂		52
CH ₃ CH ₃		43

Results

1. Temperature Dependence of the Transport Coefficients. The temperature dependence of the transport coefficients has been studied only in poly(2-ethoxy ethyl methacrylate) and in copolymer MM-70/30. The diffusion and solubility coefficients have been determined in the range 0–40 °C as our device does not permit much higher temperature increases. As shown in Figures 6 and 7, no unexpected behavior is presented by the membranes: diffusivity increases with temperature in a roughly Arrhenius fashion, and the temperature dependence of the coefficient is stronger the larger the diffusing gas (Figure 6 and Table 3). Solubility increases on lowering the temperature and more so the larger the interaction of the gas with the matrix (Figure 7, Table 3). Comparison of the data from PEEMA and copolymer MM-70/30 is in agreement with what we know about their structure: the heats of solution in the more apolar PEEMA matrix are endothermic for oxygen and nitrogen, which are not strongly interacting gases, and small and exothermic for carbon dioxide. In the case of MM-70/30, all heats of solution are exothermic in particular in the case of carbon dioxide, which possess

Table 3. Heat of Solution of the Gases in PEEMA and MM-70/30

gas	ΔH_s (kJ mol ⁻¹) PEEMA	ΔH_s (kJ mol ⁻¹) MM-70/30
O ₂	2.1	-6.7
N ₂	1.2	-3
CO ₂	-6.7	-24
CH ₄		-11.5
CH ₂ CH ₂		-8.4
CH ₃ CH ₃		-19.4

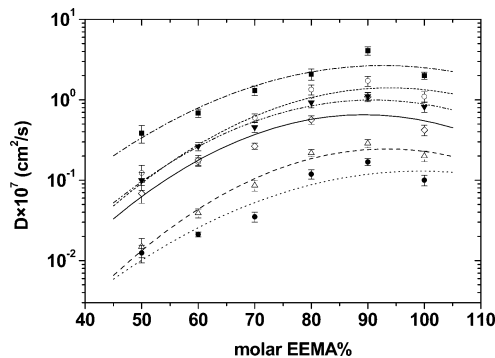


Figure 8. Diffusion coefficients as a function of the molar percentage of EEMA in each MM copolymer. The code for gases is oxygen (■), nitrogen (○), methane (◇), carbon dioxide (▼), ethane (●), and ethylene (△).

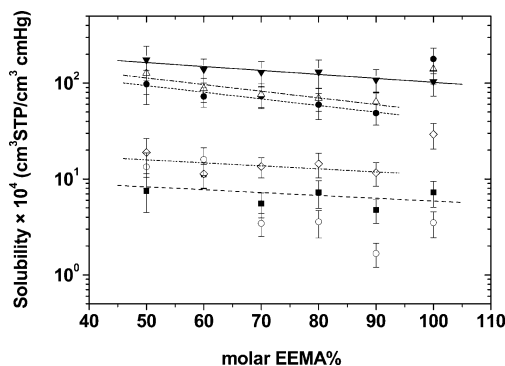


Figure 9. Solubility of gases as a function on the molar percentage of EEMA in each MM copolymer. The code for gases is oxygen (■), nitrogen (○), methane (◇), carbon dioxide (▼), ethane (●), and ethylene (△).

a permanent dipole and thus strongly interacts with polar matrixes.

2. Transport Coefficients at 35 °C and 1 Bar. The flow of He, O₂, N₂, CO₂, CH₄, CH₃CH₃, and CH₂CH₂ through our five copolymers has been measured at 35 °C and 1 bar, and the diffusivity, permeability, and solubility of each of the gases have been determined as explained in the Experimental Section. The results are shown in Figures 8–10 as a function of the molar percentage of 2-ethoxyethyl methacrylate in each copolymer. In all five copolymers at 35 °C, $D(\text{He}) > D(\text{O}_2) > D(\text{N}_2) \approx D(\text{CO}_2) > D(\text{CH}_4) > D(\text{CH}_2\text{CH}_2) > D(\text{CH}_3\text{CH}_3)$, an expected trend which is in accordance with the size of the gases. Figure 11 shows the diffusion coefficients in the five copolymers and in PEEMA as a function of the critical volume of the gas. The correlation between gas size and diffusivity is very good; the membrane with the lowest diffusion coefficients is MM-50/50, followed by MM-60/40, MM-70/30, and MM-80/20 and PEEMA, which have almost exactly the same diffusion values, and finally the highest diffusivity for all gases is that of MM-90/10. This is also seen in Figure 8: as the molar percentage of 2-ethoxyethyl methacrylate increases, so do diffusion coefficients, up to 80/20,

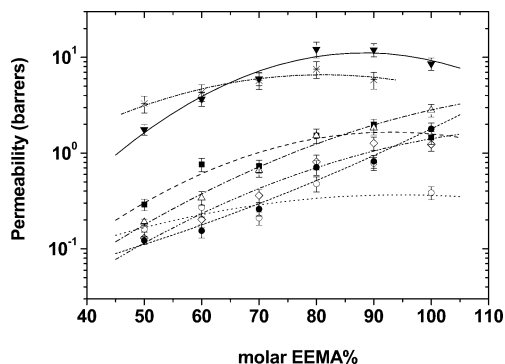


Figure 10. Permeability of the gases as a function of the molar percentage of EEMA in each MM copolymer. The code for gases is oxygen (■), nitrogen (○), methane (◇), carbon dioxide (▼), ethane (●), ethylene (△), and helium (*).

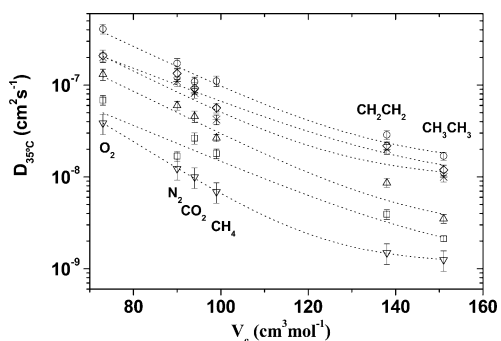


Figure 11. Diffusion coefficients of the gases in the five copolymers and in PEEMA as a function of their critical volume. The symbol code for the copolymers is MM-50/50 (▽), MM-60/40 (□), MM-70/30 (∇), MM-80/20 (◇), MM-90/10 (○), and PEEMA (*).

Table 4. Transport Coefficients of EEMA/MAG and EEMA/HEMAM at 35 °C and 1 bar

sample	$D \times 10^8$ ($\text{cm}^2 \text{s}^{-1}$)			$S \times 10^4$ ($\text{cm}^3 \text{(STP)} \text{cm}^{-3} \text{cmHg}^{-1}$)			P (barrer)		
	O ₂	N ₂	CO ₂	O ₂	N ₂	CO ₂	O ₂	N ₂	CO ₂
MM-50/50	2.7	1.4	1.2	11.2	10.8	130	0.3	0.15	1.56
MG-50/50	4.5	1.2	1.9	5.4	10	89	0.24	0.12	1.74

then diffusivity does not change much with a further increase of 2-ethoxyethyl methacrylate content.

Figure 9 shows the solubility of the studied gases in the six membranes. Solubility decreases gradually as the content of 2-ethoxyethyl methacrylate increases, the only noteworthy feature being the fact that, except for carbon dioxide, in poly(2-ethoxyethyl methacrylate) gases have a higher solubility than in any of the copolymers. It is not surprising that the presence of a polar monomer such as 2-hydroxy ethyl methacrylamide should increase the solubility of the gases in the matrix. The order of solubility coefficients is also as expected: $S(\text{CO}_2) > S(\text{CH}_2\text{CH}_2) \approx S(\text{CH}_3\text{CH}_3) > S(\text{CH}_4) > S(\text{O}_2) > S(\text{N}_2)$. Permeability, the product of diffusivity and solubility, varies as shown in Figure 10.

2-Hydroxyethyl methacrylamide has not been the only polar monomer tested. In fact, we began by synthesizing a series of copolymers of EEMA and 2,3-hydroxypropyl methacrylate (series MG). The swelling ratios of copolymers MM-50/50 and MG-50/50 are, respectively, 153% and 54%, and their transport coefficients in the solid state are compared in Table 4. Both copolymers are water swelled, more so MM-50/50, and the transport coefficients in the solid state are very similar in both of them. However, the mechanical properties of the series

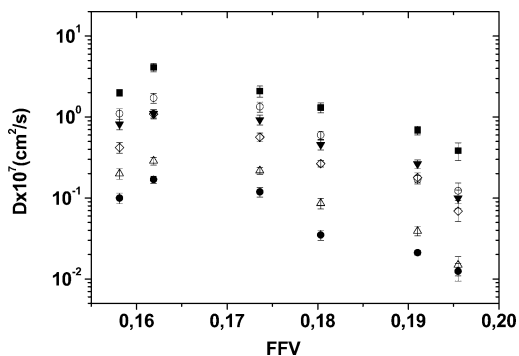


Figure 12. Diffusion coefficients as a function of the fractional free volume of each MM copolymer and of PEEMA. The code for gases is oxygen (■), nitrogen (○), methane (◇), carbon dioxide (▼), ethane (●), ethylene (△), and helium (*).

MG when unswelled were very poor, which makes the handling of the samples difficult because of their fragility as the amount of 2,3-hydroxypropyl methacrylate increased. From a practical point of view it is very desirable that membranes show both good mechanical properties in the solid state and high swelling ratio, and therefore, series MG has been for the moment disregarded. On the other hand, the series MM, even with methacrylamide molar ratios as high as 50%, has very good mechanical properties in the solid state and is readily water swelled, which is very important as diffusion coefficients in hydrogels are mostly dependent on the swelling ratio.

Discussion

Diffusion and Free Volume. Routine characterization of membranes aimed at gas transport involves mainly determination of the free volume and chain mobility in the bulk, two structural features related to diffusivity, and determination of specific interactions, which are related to solubility. As free volume and chain mobility increase, so does diffusivity, for this property is determined by the rate at which holes of adequate size are generated in the matrix. Figure 12 shows the diffusion coefficients of all the studied gases in the six membranes as a function of the fractional free volume. Surprisingly, on going from MM-50/50 to MM-80/20, as FFV decreases, diffusivity increases strongly; this is certainly not the usual behavior. On the other hand, the dependency shown by the diffusion coefficients of all the gases as a function of the glass-transition temperature of the membrane (Figure 13) follows the trend usually found in amorphous materials.

Figure 14 shows the diffusion coefficient of oxygen as a function of FFV for a number of polymers studied by us or others.^{27–32} Though scatter of the data exists, there is an inverse correlation between fractional free volume and diffusivity given by the well-known Fujita equation³³

$$D = Ae^{-B/FFV} \quad (4)$$

According to free-volume theories, $B = \gamma v^*/v_m$, where γ accounts for the overlap in free volume and varies from 0.5 to 1, v^* is the minimum critical volume needed to accommodate a diffusing molecule, and v_m is the average free volume. As a matter of fact, our five copolymers and PEEMA do not show especially anomalous diffusion coefficients when compared to other polymers. It is not the values in themselves but the

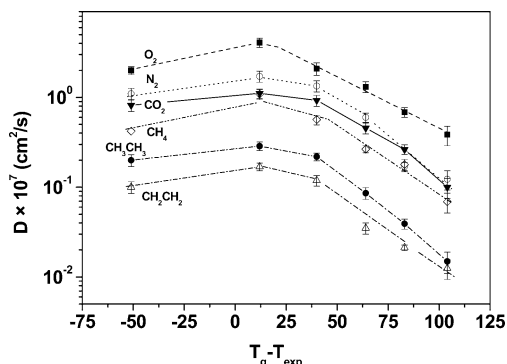


Figure 13. Diffusion coefficients as a function of the glass-transition temperature of each of the MM copolymers and of PEEMA. The code for gases is oxygen (■), nitrogen (○), methane (◇), carbon dioxide (▼), ethane (●), ethylene (△), and helium (*).

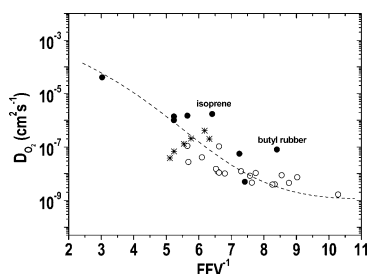


Figure 14. Diffusivity of oxygen in a set of polymers as a function of their fractional free volume at 25 °C. Membranes measured under the glass transition are represented with open symbols, membranes measured over their glass transition are represented with solid symbols, and membranes studied in this work are represented with a star.

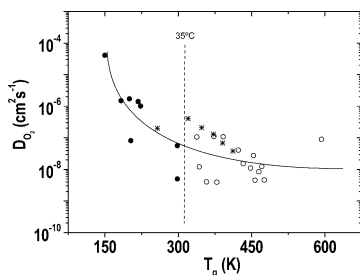


Figure 15. Diffusivity of oxygen in a set of polymers as a function of their glass transition. Membranes measured under the glass transition are represented with open symbols, membranes measured over their glass transition are represented with solid symbols, and membranes studied in this work are represented with a star.

trend with FFV shown in Figure 12, which will be explained. It seems that as the composition of the copolymer changes and the amount of polar monomer increases, some other structural changes apart from FFV take place, which causes the decrease of diffusivity even if FFV is increasing.

Diffusion and Glass Transition. Figure 15 shows the evolution of diffusivity with glass-transition temperatures in the same polymers as in Figure 13. In this case, the trend followed by our copolymers is the same as that followed by polymers as a whole: as T_g increases, the diffusivity at a given measuring temperature decreases, and this effect is more conspicuous when T_g is under the measuring temperature than when it is over. Finally, Figure 16 shows the correlation between D and T_g/FFV , and again the five copolymers lie in the normal range of values.

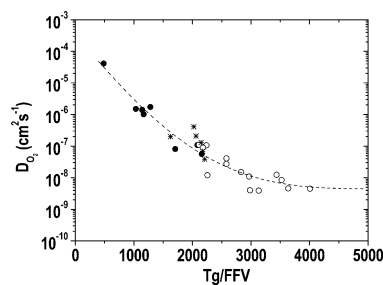


Figure 16. Diffusivity of oxygen in a set of polymers as a function of the ratio between their glass transition and fractional free volume at 25 °C. Membranes measured under the glass transition are represented with open symbols, membranes measured over their glass transition are represented with solid symbols, and membranes studied in this work are represented with a star.

As shown in the mechanodynamical spectra of Figure 2, there is only one T_g in the copolymers and no block structures or phase separation seems to exist; the structure of the membranes is homogeneous. PEEMA and MM-90/10 are measured over, and at their T_g and therefore their rubbery state could explain their high diffusivity. However, MM-80/20 has a T_g of 75 °C, and the rest of the copolymers show even higher T_g ; thus, MM-70/30 to MM-50/50 are glasses at the measuring temperature.

Diffusion and Molecular Interactions. A look at the FTIR spectra (Figures 4 and 5) shows that as the ratio between HEMAM and EEMA increases, the IR band corresponding to the C=O stretching of the amide group shifts to lower wavenumber and the band due to the stretching of the associated NH group increases with respect to the free NH group. In fact, the shift to lower wavenumber of $\nu_{\text{amide}}(\text{C}=\text{O})$ is due to the increase in a band at 1634 cm^{-1} of associated $\nu_{\text{amide}}(\text{C}=\text{O})$ and progressive disappearance of the band at 1650 cm^{-1} , related to free or less associated $\nu_{\text{amide}}(\text{C}=\text{O})$. In addition, a shoulder appears at ca. 1708 cm^{-1} due to the existence of EEMA carbonyls involved in hydrogen bonding, and this shoulder is more intense the amount of HEMAM in the copolymer. Then, as the amount of polar methacrylamide increases, the inter- or intramolecular interactions between the copolymer units, via hydrogen bonding between NH and CO groups, increases, leading to a stiffer molecular structure. This is the origin of the strongly positive deviation of T_g shown in Figure 3 and most probably also of the decrease in diffusivity shown in the glassy copolymers MM-80/20 to MM-50/50. That MM-90/10 shows the normal trend in the correlation between FFV and D with respect to PEEMA is probably due to the fact that when considerable cooperative chain motions exist, the intermolecular interactions must be partly or totally released; in fact, the IR spectrum of MM-90/10 is very different from that of the other copolymers, both in the position of the $\nu(\text{C}=\text{O})_{\text{amide}}$ and in the very low intensity of the band due to interacting NH groups. Therefore, as the amount of HEMAM in the copolymer increases, the structure changes from flexible and apolar to stiff and polar and as a result diffusivity decreases even if FFV increases.

Diffusion and Cohesive Energy Density. In 1954 Meares proposed that the diffusion of a penetrant through a glassy matrix could be viewed as a jump motion between neighboring holes through channels large enough to constitute an adequate passageway.³³ This is also the picture derived from MD simulation of

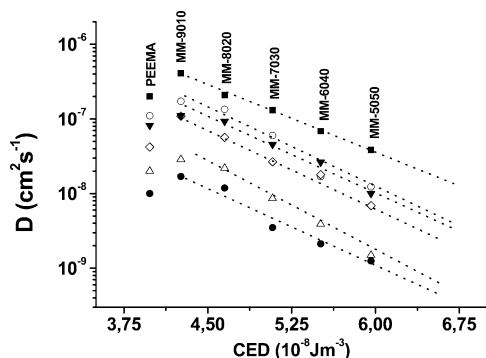


Figure 17. Diffusion coefficients as a function of cohesive energy density of each of the MM copolymers and of PEEMA. The code for gases is oxygen (■), nitrogen (○), methane (◇), carbon dioxide (▼), ethane (●), and ethylene (△).

the diffusional process. Thus, the diffusional process is governed by both the number and size of the holes and the energy required to open a passageway between them. The number and size of the “holes” in the materials is quantified by determining the free volume in the matrix, while the activation energy of the channel opening was equated by Meares to the product of the passageway volume and the polymer cohesive energy density CED

$$E_D = \frac{1}{4} \pi d^2 \alpha \cdot \text{CED} \cdot N_A \quad (5)$$

In this equation the passageway is taken as a cylinder of the same diameter d as the penetrant and of length α , which is the length of the diffusional step. Cohesive energy density is, together with the fractional free volume, a parameter strongly related to the diffusional process.^{30,34,35}

Figure 17 shows the diffusion coefficient of the gases studied in this work as a function of the CED of each of our polymers. Equation 5 proposes a relationship between E_D and CED and not between D and CED; however, there is experimental evidence³³ that D_0 and E_D are directly related, and therefore, the correlation between E_D and CED should also qualitatively hold for D and CED. The CED of our polymers has been estimated by a group contribution method.³⁶ The diffusion coefficients of the five copolymers decrease as their CED increases (Figure 17); the progressive incorporation of 2-hydroxyethyl methacrylamide in the copolymer makes the intermolecular interactions stronger and thus the structure stiffer and characterized by higher CED values. Under these conditions the creation of a channel between microcavities becomes progressively more difficult. By stiffer it is meant both that the glass transition shifts to higher temperatures and that less sub- T_g relaxations are found. These local sub- T_g motions are known to contribute largely to the molecular diffusion in glasses, as, for example, they make the creation of a channel or passageway easier. It is noteworthy that as for the effect of the matrix CED on the diffusion coefficients of the gases, the homopolymer PEEMA does not seem to belong to the same series as the other five copolymers. In recent work,³⁷ it has been proposed that the scatter in the correlation between diffusion coefficients and fractional free volume is related to the CED of each polymeric matrix. In fact, a representation of the logarithmic deviation (defined as the difference between the logarithm of the experimental diffusion

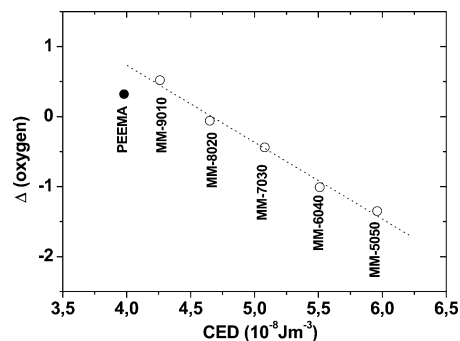


Figure 18. Logarithmic deviation between the oxygen diffusion coefficients as a function of the CED of each MM copolymer. Open symbols correspond to copolymers measured under their T_g ; solid symbols correspond to copolymers measured over their T_g .

coefficient and the logarithm diffusion coefficient of the corresponding fit) vs CED of the different polymers yielded very reasonable straight lines for a number of gases. The same data treatment has been performed with our data, representing the logarithmic deviation of the oxygen diffusion coefficient as obtained from Figure 14. This is represented in Figure 18. As in the work cited before,³⁷ the good correlation shown in Figure 18 strongly supports that the scatter of the data when representing $\log D$ as a function of the inverse of FFV is clearly related to the different CEDs of the polymeric matrixes studied. This scatter due to CED does not mean that free volume theories have to be abandoned in the interpretation of transport data; as explained by Nagel et al.,³⁷ the dependence on CED can be contained in the prefactor of the Fujita equation.

As for applications, all the methacrylic copolymers from MM-80/20 to MM-50/50 have good mechanical properties in the solid state, are not fragile at room temperature, show moderately high glass-transition temperatures, form transparent membranes, and have high swelling ratio. These solid methacrylic matrixes are appropriate to be used in the development of soft contact lenses;³⁸ thus, it is envisaged to measure oxygen permeability in the corresponding hydrogels.

Conclusions

The transport properties of a series of methacrylic copolymers prepared by radical polymerization of the monomers 2-ethoxyethyl methacrylate and 2-hydroxyethyl methacrylamide and a small quantity of a cross-linking agent, ethylene glycol dimethacrylate, have been studied. Water swelling of the membranes, mechanodynamical analysis, density measurements, and ATR-FTIR studies have been performed on the copolymers. The cohesive energy density has also been estimated. As the amount of monomer 2-[(methacryloyloxy)amino]ethanol increases, FFV, CED, swelling ratio, and T_g increase while diffusivity and permeability decrease strongly. A linear relationship exists between the logarithmic deviation of the diffusion coefficients and CED. The development of strong specific intermolecular interactions involving the amide groups and accordingly a stiffer chain structure are responsible for the decrease in diffusivity and the large positive deviation from the Fox equation of the studied copolymers.

Even if the structure becomes stiffer, copolymers with a large amount of 2-hydroxyethyl methacrylamide show good mechanical properties in the solid state together

with a high swelling ratio, which makes them adequate for the development of contact lenses.

Acknowledgment. We would like to acknowledge financial support from the Junta de Castilla y León (Bu16/02) and the Ministerio de Ciencia y Tecnología (MAT2002-02502, MAT2002-04042-c02-02).

References and Notes

- (1) Koros, W. J.; Fleming, G. K. *J. Membr. Sci.* **1993**, *83*, 1
- (2) Kesting, R. E.; Fritze, A. K. *Polymeric Gas Separation Membranes*; John Wiley and Sons: New York, 1993.
- (3) *Polymer Membranes for gas and vapor separation*; Freeman, B. D., Pinnau, I., Eds.; ACS Symposium series 733; American Chemical Society: Washington, D.C., 1999; Chapter 1.
- (4) Stern, S. A. *J. Membr. Sci.* **1994**, *94*, 1.
- (5) Nunes, S. P.; Peinemann, K. V. *Membrane Technology in the Chemical Industry*; Wiley-VCH: New York, 2001.
- (6) *Basic Principles of Membrane Technology*, 2nd ed.; Marcel Mulder, Kluwer Academic Publishers: New York, 1996.
- (7) *Membrane formation and Modification*; Pinnau, I., Freeman, B. D., Eds.; ACS Symposium Series 744; American Chemical Society: Washington, D.C., 1999.
- (8) George, S. C.; Thomas, S. *Prog. Polym. Sci.* **2001**, *26*, 985.
- (9) Pandey, P.; Chauhan, R. S. *Prog. Polym. Sci.* **2001**, *26*, 853.
- (10) Meyer, W. H. *Adv. Mater.* **1998**, *10*, 439.
- (11) Dias, F. B.; Plomp, L.; Veldhuis, J. B. *J. Power Sources* **2000**, *88*, 169.
- (12) Tiemblo, P.; Fernández-Arizpe, A.; Riande, E.; Guzmán, J. *Polymer* **2003**, *44*, 635.
- (13) Tiemblo, P.; García, F.; García, J. M.; García, C.; Riande, E.; Guzmán, J.; *Polymer* **2003**, *44*, 2661.
- (14) Tiemblo, P.; Guzmán, J.; Riande, E.; García, F.; García, J. M. *Polymer* **2003**, *44*, 6773.
- (15) Habaue, S.; Morita, M.; Okamoto, Y. *Macromolecules* **2002**, *35*, 2432.
- (16) Feng, X.; Yan, L.; Wen, J. Pan, C. *Polymer* **2002**, *43*, 3131.
- (17) Percec, V.; Randall, R. *Macromolecules* **1989**, *22*, 4408.
- (18) Privalko, V. P.; Khaenko, E. S.; Grekov, A. P.; Savelyev, Yu. *Polymer* **1994**, *35*, 1730.
- (19) Nishide, H.; Kawakami, H.; Suzuki, T.; Azechi, Y.; Soejima, Y.; Tsuchida, E. *Macromolecules* **1991**, *24*, 6306.
- (20) Nishide, H.; Ohyanagi, M.; Okada, O.; Tsuchida, E. *Macromolecules* **1986**, 495–496.
- (21) Nishide, H.; Ohyanagi, M.; Okada, O.; Tsuchida, E. *Macromolecules* **1987**, 417–422.
- (22) Wang, C.; Chen, C.; Cheng Huang, C.; Chen, C. Y.; Kuo, J. F. *J. Membr. Sci.* **2000**, *177*, 189.
- (23) Kosvintseva, S. R.; Riande, E.; Velarde, M. G.; Guzmán, J. *Polymer* **2001**, *42*, 7395.
- (24) García, F.; de la Peña, J. L.; Delgado, J. J.; García, N.; Guzman, J.; Riande, E.; Calle, P. *J. Polym. Sci., Part A: Polym. Chem.* **2001**, *39*, 1843.
- (25) *Hyperchem, Computational Chemistry*, Version 5.01; Hypercube Inc.; Ontario, Canada, 1999.
- (26) Laguna, M. F.; Guzmán, J.; Riande, E.; Saiz, E. *Macromolecules* **1998**, *31*, 7488.
- (27) Xuesong, G.; Feng, L. *Polymer* **1995**, *36*, 1035.
- (28) Stannet, V.; Williams, J. L. *J. Polym. Sci., Part C* **1965**, 45–49.
- (29) Shelby, J. E. *Handbook of Gas Diffusion in Solids and Melts*; ASM International: 1996; Chapter 6.
- (30) Thran, A.; Kroll, G.; Faupel, F. *J. Polym. Sci., Part B: Polym. Phys.* **1999**, *37*, 3344.
- (31) Tiemblo, P.; Guzmán, J.; Riande, E.; Mijangos, C.; Reinecke, H. *Polymer* **2001**, *42*, 4817 and corrigendum *Polymer* **2001**, *42*, 8321.
- (32) Costello, L. M.; Koros, W. J. *J. Polym. Sci., Part B: Polym. Phys.* **1995**, *33*, 135.
- (33) Kumins, C. A.; Kwei, T. K. *Diffusion in Polymers*; Crank, J., Park, G. S., Eds.; Academic Press: New York, 1968; Chapter 4, pp 108–123 and references therein.
- (34) Liu, R. Y. F.; Hiltner, A.; Baer, E. *J. Polym. Sci., Part B: Polym. Phys.* **2004**, *42*, 493 and references therein.
- (35) Alentiev, A. Yu; Yampolskii, Y. P. *J. Membr. Sci.* **2002**, *206*, 291.
- (36) Van Krevelen, D. W. *Properties of Polymers: Their correlation with chemical structure; their numerical estimation and prediction from additive group contributions*, 3rd ed.; Elsevier: New York, 1990; pp 535–582.
- (37) *Polymers. Biomaterials and medical applications*; Krosschwitz, J. I., Ed.; Encyclopedia Reprint Series; John Wiley and Sons: New York, 1989; p 99.
- (38) Nagel, C.; Gunther-Schade, K.; Fritsch, D.; Strunskus, T.; Faupel, F. *Macromolecules* **2002**, *35*, 2071.

MA049945H